Am J Physiol Renal Physiol 310: F259–F271, 2016.
First published November 25, 2015; doi:10.1152/ajprenal.00389.2015.

Remote effects of acute kidney injury in a porcine model

David S. Gardner,[1] Simone De Brot,[1] Louise J. Dunford,[1,3] Llorenc Grau-Roma,[1] Simon J. M. Welham,[2] Rebecca Fallman,[1] Saoirse E. O'Sullivan,[4] Weng Oh,[3] and Mark A. J. Devonald[1,3]

[1]*School of Veterinary Medicine and Science, University of Nottingham, Loughborough, United Kingdom;* [2]*School of Biosciences, University of Nottingham, Loughborough, United Kingdom;* [3]*Renal and Transplant Unit, Nottingham University Hospitals NHS Trust, Nottingham, United Kingdom; and* [4]*School of Graduate Entry Medicine and Health, Royal Derby Hospital, Derby, United Kingdom*

Submitted 3 September 2015; accepted in final form 19 November 2015

Gardner DS, De Brot S, Dunford LJ, Roma LG, Welham SJ, Fallman R, O'Sullivan SE, Oh W, Devonald MA. Remote effects of acute kidney injury in a porcine model. *Am J Physiol Renal Physiol* 310: F259–F271, 2016. First published November 25, 2015; doi:10.1152/ajprenal.00389.2015.—Acute kidney injury (AKI) is a common and serious condition with no specific treatment. An episode of AKI may affect organs distant from the kidney, further increasing the morbidity associated with AKI. The mechanism of organ cross talk after AKI is unclear. The renal and immune systems of pigs and humans are alike. Using a preclinical animal (porcine) model, we tested the hypothesis that early effects of AKI on distant organs is by immune cell infiltration, leading to inflammatory cytokine production, extravasation, and edema. In 29 pigs exposed to either sham surgery or renal ischemia-reperfusion (control, $n = 12$; AKI, $n = 17$), we assessed remote organ (liver, lung, brain) effects in the short (from 2- to 48-h reperfusion) and longer term (5 wk later) using immunofluorescence (for leukocyte infiltration, apoptosis), a cytokine array, tissue elemental analysis (e.g., electrolytes), blood hematology and chemistry (e.g., liver enzymes), and PCR (for inflammatory markers). AKI elicited significant, short-term (~24 h) increments in enzymes indicative of acute liver damage (e.g., AST:ALT ratio; $P = 0.02$) and influenced tissue biochemistry in some remote organs (e.g., lung tissue [Ca^{2+}] increased; $P = 0.04$). These effects largely resolved after 48 h, and no further histopathology, edema, apoptosis, or immune cell infiltration was noted in the liver, lung, or hippocampus in the short and longer term. AKI has subtle biochemical effects on remote organs in the short term, including a transient increment in markers of acute liver damage. These effects resolved by 48 h, and no further remote organ histopathology, apoptosis, edema, or immune cell infiltration was noted.

AKI; ischemia-reperfusion; distant effects; cytokines; apoptosis

ACUTE KIDNEY INJURY (AKI) is a common and serious condition with no specific treatment (2). The prevalence and cost of AKI was recently estimated at 14.1% of all in-patients to a universal healthcare system (National Health Service, UK) and £1.02 billion/yr for in-patient care (25). A single episode of AKI requiring hospital admission increases the risk of subsequent chronic kidney disease (CKD) or cardiovascular disease long after recovery from the original insult (5, 7, 21). AKI can precipitate or aggravate other conditions that may have significant impact on an individual's morbidity and life expectancy.

One example of the diverse clinical complications that may ensue after an episode of AKI is the increased risk of nonrenal organ injury (17). Experimental studies have shown that AKI is associated with mild-to-moderate acute injury in organs distant from the kidney such as the liver (16, 24, 28), lung (19, 34), and brain (6, 30): the "remote or distant organ effects of AKI." Ischemic kidney damage is characterized by apoptosis and necrosis of proximal tubular epithelial cells (40). Consequences of such programmed and necrotic cell death in the kidney include activation of the innate immune system by regional hypoxia and local cellular debris, evoking a pathogen- and/or damage-associated molecular pattern (PAMP and/or DAMP) (4, 40) inducing local infiltration of immune cells into the tissue and concomitant increased inflammatory cytokine production (e.g., IL-1β) (e.g., neutrophils, macrophages). Acute loss of proximal tubular epithelial cells, rich in mitochondria (9, 10), electrolytes (e.g., Ca^{2+}), and trace elements (e.g., Fe^{2+}) (41, 42) causes local biochemical and mineral imbalance that may activate local pathophysiological events (1, 32, 41). These localized effects may provoke a systemic reaction, resulting in pathophysiological sequelae in distant organs, most often characterized by infiltration with immune cells, extravasation leading to edema and ultimately, apoptosis (11, 19, 28, 40). For example, AKI leads to an increased susceptibility to respiratory failure (12), acute liver damage (marked by altered liver enzymes, inflammatory cell infiltration) (16) and functional impairment of the brain (e.g., with increased vascular permeability) (30). Swine are excellent biomedical models for human, particularly renal, disease (37), as their size, anatomy, and physiology are alike (15). The porcine immune system is also very similar to that of humans (31). These are important considerations in recapitulating and extrapolating from an animal model to a clinical disease such as AKI. We have developed and characterized a preclinical animal (porcine) model of mild-moderate AKI (14). Here, we extend this model, to examine potential remote effects on other organs (e.g., liver, lung, and brain) in the short and longer term. To our knowledge, no study has considered potential remote effects of AKI in a large-animal model nor across multiple organs in the same individual. We hypothesize that organ cross talk after AKI in swine, as in murine models, is initiated early in the course of an acute disease by infiltration of remote organs with immune cells, leading to increased cytokine production, cellular extravasation, edema, and apoptosis.

To address this hypothesis, we *1*) used biobanked tissue from our previously established porcine model of mild-moderate ischemia-reperfusion (IR) AKI (14) and *2*) conducted new studies in subsets of control and AKI pigs using an identical experimental design for collection and analysis of whole blood. We first characterized a time course of immune cell activation after whole blood sampling (0–24 h) using hematology and flow cytometry and then assessed possible immune cell infiltration in the kidney and other organs (liver,

Address for reprint requests and other correspondence: D. Gardner, School of Veterinary Medicine and Science, Univ. of Nottingham, Sutton Bonington Campus, Loughborough LE12 5RD, UK (e-mail: david.gardner@nottingham.ac.uk).

lung, and hippocampus) as follows: *1*) visual assessment of hematoxylin- and eosin (HE)-stained sections by two experienced veterinary pathologists, *2*) immunohistofluorescence using porcine-specific antibodies, *3a*) quantification of protein abundance (porcine-specific Milliplex array), and *3b*) mRNA expression (qRT-PCR) of selected cytokines. The possibility of low-grade tissue injury or subcellular biochemical effects in remote organs was assessed by quantifying a time course in plasma of liver injury markers (e.g., transferase enzymes) alongside characterization of the tissue composition of electrolytes, minerals, trace elements, and water content at 48 h and 5 wk post-IR injury. As an early indicator of significant cellular damage, we used the terminal deoxynucleotidyl transferase dUTP nick end labeling ($TUNEL^{+ve}$) technique to identify an increase in apoptotic cell number at remote sites.

METHODS

Animals and Experimental Design

All procedures were performed in accordance with the UK Animals (Scientific Procedures) Act (1986) and were approved by the local ethical review committee of the University of Nottingham. Thirty-five female pigs were randomly assigned (sealed envelope) to either a sham-control ($n = 15$) or IR ($n = 20$) protocol (weights; 55–65 kg). All pigs were anesthetized for general surgery, details of which including the analgesic regime, have been previously described (14). In brief, a venous catheter was inserted for supportive fluid delivery and vascular access. IR-induced AKI was experimentally reproduced through bilateral renal artery cross-clamping (40 min) with 48-h postsurgical recovery. Time zero was considered to be the time of atraumatic vascular clamp removal. Sham-controls experienced all procedures except renal artery clamping. Blood was collected at intervals, and plasma was biobanked at −20°C for further analysis. At 48 h, control ($n = 12$) or IR ($n = 17$) pigs were humanely euthanized by a lethal dose of barbiturate (200 mg/kg), and samples of kidney (cortex), liver (dorsal aspect of right lobe), lung (right lobe), and whole hippocampus (from right cerebral hemisphere) were obtained. Remaining control ($n = 3$) or IR ($n = 3$) pigs were euthanized at 5 wk postsurgery, a time post-IR injury when significant organ histopathological changes as a result of immune cell infiltration should be apparent after AKI. Tissue samples were either snap-frozen in LN_2 or super-cooled isopentane, before embedding in optimal cutting temperature (OCT) or fixed in 4% paraformaldehyde (24 h at 4°C) and subsequently preserved in wax after 24-h rinsing in 0.02 M PBS.

Blood Hematology, Tissue Biochemistry, and Histology

Plasma markers of acute liver injury were measured by autoanalyzer using colorimetric enzymatic techniques (RX-Imola, Randox, County Antrim, UK). All study samples were randomly distributed over three separate RX-Imola assays. Typical interassay variation was <5% for aspartate aminotransferase (AST; IU/l), alanine aminotransferase (ALT; IU/l), γ-glutamyltransferase (GGT; IU/l), alkaline phosphatase (ALP; IU/l), total bilirubin (μmol/l), and glutamate dehydrogenase (GLDH; IU/l). Hematology was conducted on freshly collected (Li-Hep tubes) whole blood samples using a Medonics CA620 (Menarini; Wokingham, UK) or by flow cytometry (BD FACS-Canto II) using mouse, anti-pig FITC antibodies for neutrophil-derived granulocytes (ID: MCA2599F), monocyte-derived dendritic cells ($CD172a^+$, ID: MCA2312F), or total T-helper cells ($CD4a^+$, ID: MCA1749F) all purchased from AbD Serotec (Kidlington, UK). In brief, 25 μl whole blood was incubated with each cell type-, porcine-specific antibody for 30 min. Red blood cells were then lysed using 5 ml ammonium chloride-potassium carbonate lysis buffer, centrifuged, and the pellet was resuspended in 300 μl PBS. The cell suspension was analyzed by FACS to determine the relative proportions of labeled cells. Cell counts were gated at 20,000 events. Tissue elemental composition [μg/g of dry matter (DM)] was determined by inductively coupled plasma mass spectrometry (ICP-MS; XSeries II, Thermo Fisher), with intra-assay variability being <2%. A known weight of organ tissue was first freeze dried to determine the percentage of water content and subsequently digested using 2% nitric acid as previously described (18). Certified reference material (NIST SRM bovine liver, 1577c) was used to validate elemental recovery and to correct for any batch variation. Tissue cytokines were measured using a porcine-specific cytokine array (Milliplex PCYTMAG-23K, Merck Millipore) on a Magpix analyzer (Luminex) after homogenization and subsequent lysis of tissue using a bead-beater (in RIPA buffer containing protein and phosphatase inhibitors; Roche). Protein concentration (mg/ml) of the lysate was determined using a Bradford reagent. The extent of tissue apoptosis was determined by immunofluorescence using a cell-death detection kit for $TUNEL^{+ve}$ cells (Roche). Cells were visualized through a FITC filter on a Nikon Eclipse 80i microscope with a DS-Qi1Mc digital camera. Propidium iodide (PI) or 4′,6-diamidino-2-phenylindole (DAPI) were used as nuclear markers. Fixed (HE) or frozen (immunohistochemistry) tissue samples were sectioned at 5 μm, and histopathology or immunohistofluorescence was conducted using standard laboratory protocols. Briefly, antibodies against swine leucocyte antigen class II DR (SLA; MCA2314GA) were purchased from AbD Serotec (Oxford, UK). Sequence specificity for the protein of interest was >95% in each case. Primary antibodies were used after heat-mediated antigen retrieval at a concentration of 1:100, with blocking by 10% neutral goat serum and sections incubated overnight at 4°C. Secondary antibody was added (Alexa Fluor 544 used at 1:300 or Texas Red Goat anti-mouse at 1:300 dilution; Invitrogen), incubated for 1 h at room temperature followed by ×3 washes with Tris buffer. Sections were mounted with Vectashield containing DAPI and visualized as described previously (14).

Quantitative PCR

Total RNA was extracted using an RNeasy Mini Kit (Qiagen), and cDNA was synthesized using an Omniscript reverse transcriptase kit (Qiagen). Primers (Eurofins MWG, Ebersberg, Germany) were designed using NCBI Primer-BLAST and are given in Table 1. cDNA was added to each reaction, and quantitative (q) PCR was performed using a QuantiTect SYBR Green RT-PCR Kit (Qiagen) on a Roche Lightcycler 480. Melt curves were used to confirm reaction specificity. Three genes were tested for suitability as a housekeeping gene (i.e., not influenced by treatment; β-actin, cyclophilin, and 18S). In all cases, β-actin was expressed at similar levels as the target gene, was unaffected by treatment, and thus was chosen as the gene to correct for mRNA quantities. Nevertheless, in all cases, expression data were similar whether correcting to

Table 1. *Primer details for quantitative PCR (Roche Lightcycler)*

Primer		Sequence 5′ to 3′	Annealing Temperature, °C
18S	F	GATGCGGCGGCGTTATTCC	56
	R	CTCCTGGTGGTGCCCTTCC	
β-Actin	F	GGACCTGACCGACTACCTCA	56
	R	GCGACGTAGCAGAGCTTCTC	
Cyclophilin A (PPIA)	F	GCACTGGTGGCAAGTCCAT	56
	R	AGGACCCGTATGCTTCAGGA	
TGF-β1	F	TTACAACAGTACCCGCGACC	53
	R	ATTTGGTTGCCGCTTTCCAC	
TNF-α	F	GCCCTTCCACCAACGTTTTC	53
	R	TCTGGCAAGGGCTCTTGATG	

Primers were designed using NCBI/Primer-BLAST. F, forward primer; R, reverse primer; PPIA, peptidylprolyl isomerase A (cyclophilin A); TGF-β1, transforming growth factor-β1; TNF-α, tumour necrosis factor-α.

cyclophilin or 18S. qPCR was conducted on a Roche Lightcycler 480 using advanced relative quantification software.

Remote Organ Histopathology

Stained (HE) representative sections of liver, lung, and hippocampus from $n = 10$ control and $n = 10$ IR-AKI pigs were assessed independently and blindly by two European College of Veterinary Pathologists (ECVP) board-certified veterinary pathologists. All histopathology of sections was scored on a discrete scale as (−/+/++/+++) representative of any organ-specific lesions being either absent, mild (<10% of section), moderate (11–49% of section), or severe (>50% of section), respectively. For analysis, scores were numerically categorized as 0/1/2/3.

Liver histopathology. HE sections (5 μm) of liver were assessed regionally (serosal surface, portal, midzonal, and centrilobular areas, sinusoids, interstitium, bile ducts, blood and lymph vessels) for edema, hyperemia, congestion, vascular lesions, hepatocellular degeneration, intravascular leukocytosis, and tissue inflammatory cell infiltration (e.g., eosinophils, lymphocytes, macrophages, neutrophils, and plasma cells). Any apparent microscopic abnormalities for each slide were noted, e.g., vascular or lymphatic congestion or thinned hepatic cords.

Lung histopathology. HE sections (5 μm) of lung were examined regionally [serosal surface, bronchi, bronchioles, alveoli, interstitium, blood and lymph vessels, bronchial-associated lymphoid tissue (BALT)] for edema, hyperemia, congestion, vascular lesions, bronchial/bronchiolar/alveolar cellular degeneration, intravascular leukocytosis, tissue inflammatory cell infiltration (e.g., eosinophils, lymphocytes, macrophages, neutrophils, and plasma cells), and BALT hyperplasia. Any apparent microscopic abnormalities for each slide were noted, e.g., mild to moderate and multifocal expansion of interalveolar septae.

Hippocampal histopathology. HE (5 μm) sagittal sections of hippocampus were examined for edema, hyperemia, congestion, vascular lesions, neuronal degeneration, extracellular vacuolization (spongiosis), intravascular leukocytosis, and tissue inflammatory cell infiltration (e.g., eosinophils, lymphocytes, macrophages, neutrophils, and plasma cells). Any apparent microscopic abnormalities for each slide were noted.

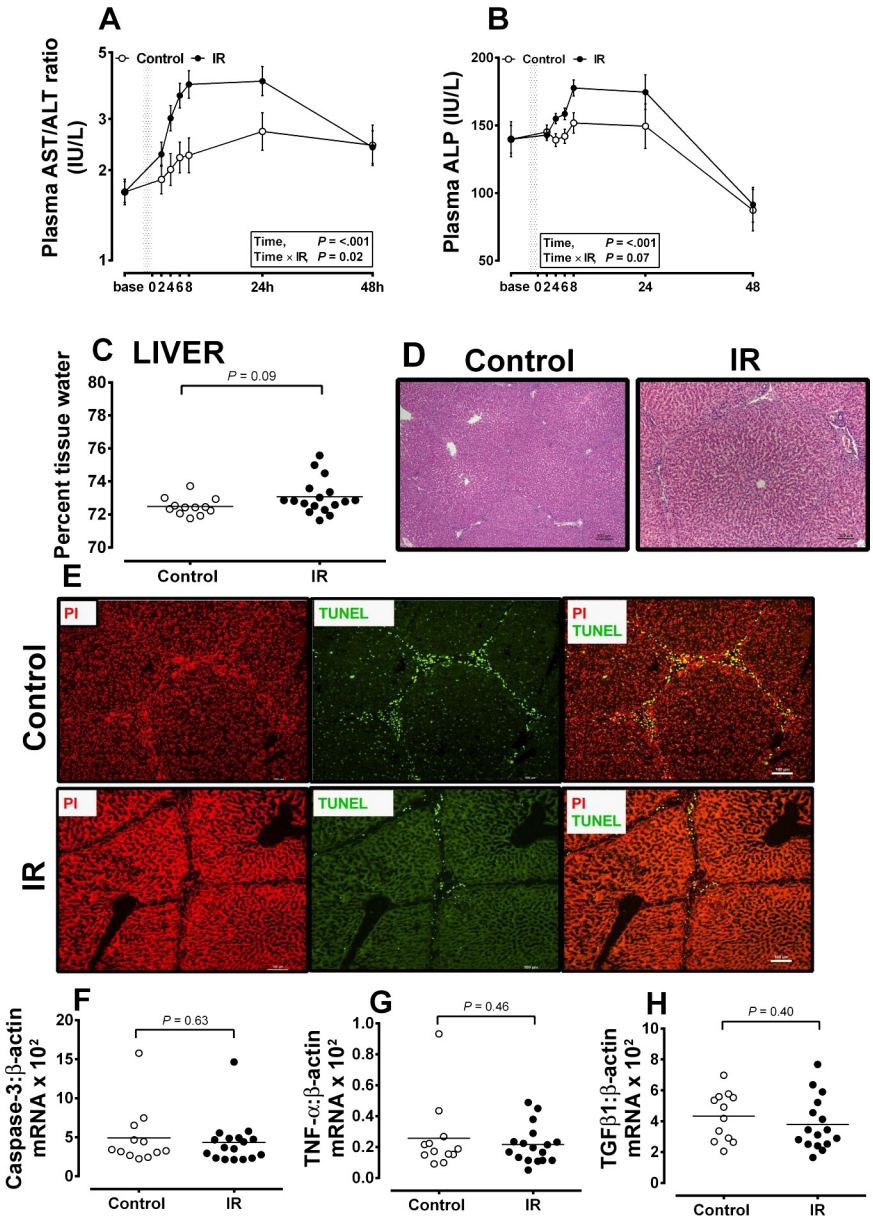

Fig. 1. Remote effects of acute kidney injury (AKI) on the liver. Renal ischemia-reperfusion (IR) injury leads to a greater increment in liver transferase enzymes, but few other hepatic effects are noted. *A* and *B*: plasma markers of acute liver injury were assayed in 100 μl plasma by autoanalyzer (RX-Imola). AST, aspartate aminotransferase; ALT, alanine aminotransferase. *C*: percentage of tissue water calculated after freeze drying a known weight of liver tissue. *D*: microphotographs (×20 objective) of hematoxylin- and eosin (H&E)-stained liver section (5 μm) for a representative control and IR pig. *E*: immunofluorescence of a single representative section (5 μm) for control and IR pigs using propidium iodide (PI) to label nuclei and a terminal deoxynucleotidyl transferase dUTP nick end labeling (TUNEL) Cell-Death Detection Kit (Roche) to fluorescently label apoptotic nuclei. Sections were captured using a FITC filter on a Nikon Eclipse 80i microscope with a DS-Qi1Mc digital camera. *F–H*: dot plots of gene expression data (qPCR) corrected to β-actin (similar results obtained after correcting to 2 other housekeeping genes, 18S and cyclophilin A) for a marker of apoptosis (caspase-3), a proinflammatory cytokine (TNF-α), and a growth factor [transforming growth factor (TGF)-β1] reported to upregulate upon acute injury. Unless otherwise stated, horizontal lines are mean with vertical lines ± estimated SE (ESE) for control ($n = 12$) and IR ($n = 17$). Quantitative data were analyzed by ANOVA for the fixed effect of treatment (control vs. IR) with or without time as a within-animal repeated measure, as appropriate. Statistical significance was accepted at $P < 0.05$.

Statistical Analysis

Continuous data (e.g., enzymatic markers of liver injury) were analyzed by one-way analysis of variance (control vs. IR) with time (0–48 h) as a within-animal repeated measure. Appropriateness of each statistical comparison was assessed by visualizing histograms of residuals and further residual (on *y*-axis) plots of *1*) fitted values and *2*) expected normal quantiles. Nonparametric datasets (i.e., those with skewed residual errors) were analyzed after $\log_{10}$ transformation. Histopathological data were analyzed by ordinal regression if variation attributable to treatment group was noted. Data are presented as means with estimated SE of the differences between means (SED) used to represent the error between statistical comparisons, unless otherwise indicated. Confidence intervals (95%) may be approximated from the normally distributed data as the means ± 2 SED. We considered $P \leq 0.050$ as indicating statistical significance. For some analyses, such as flow cytometry and hematology, only a subsample of the biological replicates could be measured. Hence, the appropriate experimental *n* for each comparison is indicated in table and figure legends. All data were analyzed using Genstat v16 (VSNi, Rothampsted, UK).

RESULTS

Remote Effects of AKI on Histopathology of the Liver, Lung, and Hippocampus at 48 Hours

Forty minutes of bilateral renal artery occlusion led to an increase (48%) in plasma creatinine that peaked at 24 h (baseline, 136 ± 31 vs. 202 ± 30 μmol/l; $P = 0.01$) and an increase in the urinary albumin:creatinine ratio (ACR) that peaked at 2 h [baseline, 16.9 (12–32) vs. 76.2 (42–114) mg/mmol creatinine, median (interquartile range); $P = 0.01$]. These reported changes are similar to those reported previously by us (14) and are consistent with moderate AKI. In remote tissues, AKI had a small, statistically nonsignificant, effect on liver tissue water content but induced a significant increment in

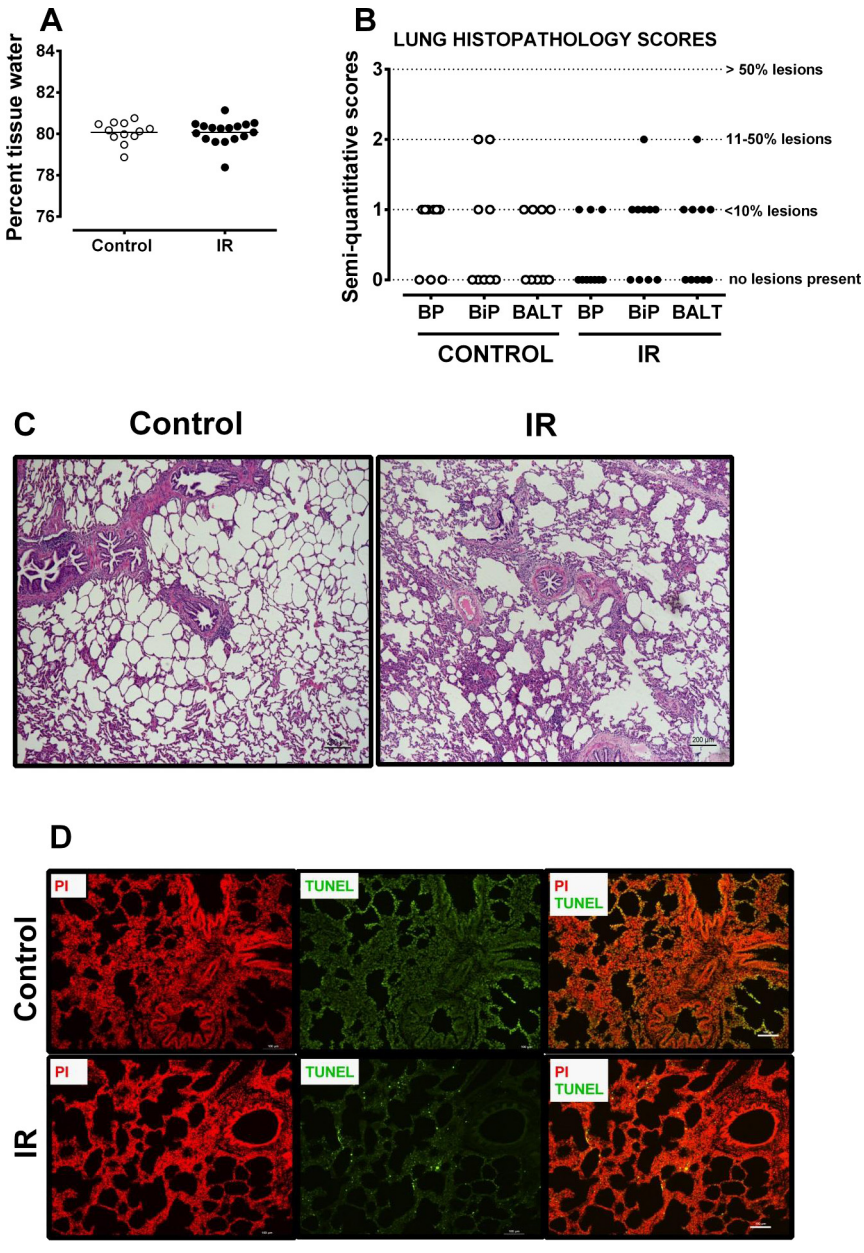

Fig. 2. Remote effects of AKI on the lung. Renal IR injury has no effect on the lung in the short term. *A*: percentage of tissue water calculated after freeze drying a known weight of lung tissue. *B*: semiquantitative pathologist score of mild-moderate lesions in the lung; BP, bronchopneumonia; BiP, bronchointerstitial pneumonia; BALT, bronchial-associated lymphoid tissue hyperplasia. *C*: microphotographs (×20 objective) of H&E-stained lung section (5 μm) for a representative control and IR pig. *D*: immunofluorescence of a single representative section (5 μm) for a control and IR pig using PI to label nuclei and a TUNEL Cell-Death Detection Kit (Roche) to fluorescently label apoptotic nuclei. Sections were captured using a FITC filter on a Nikon Eclipse 80i microscope with a DS-Qi1Mc digital camera.

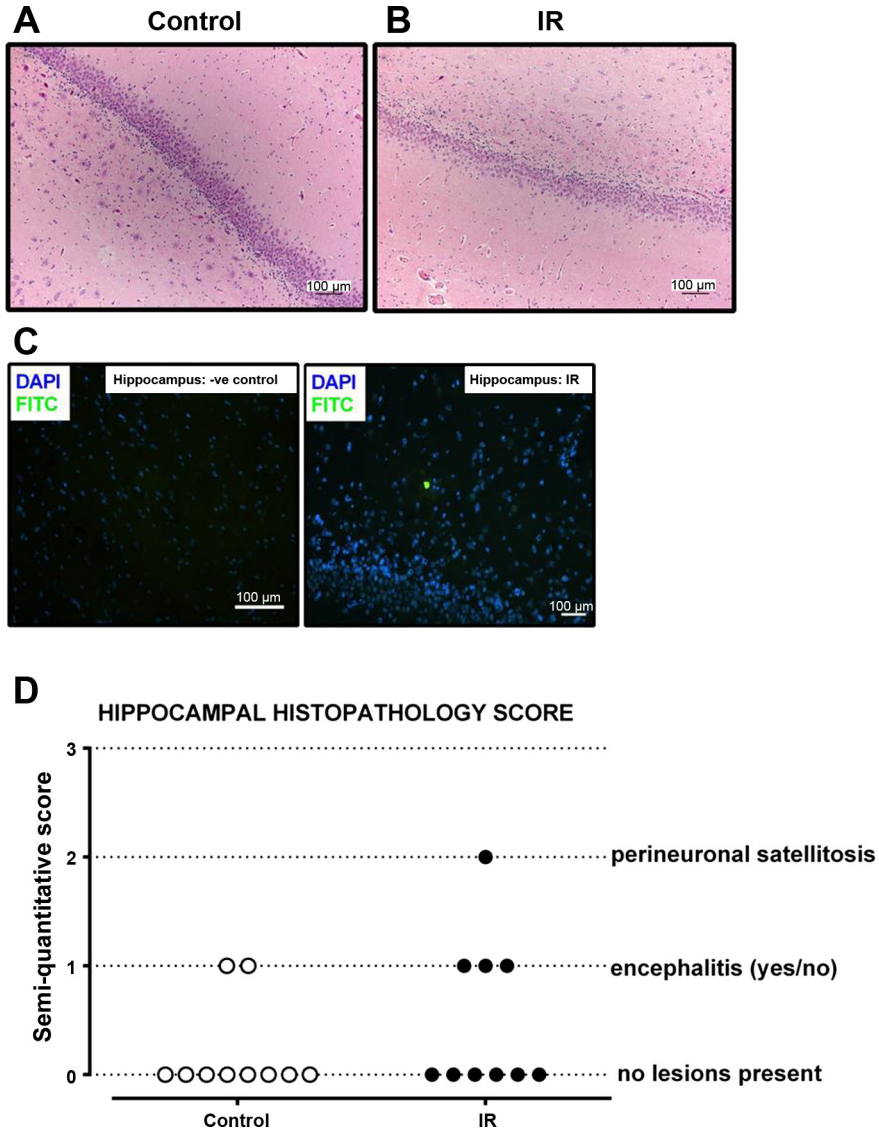

Fig. 3. Remote effects of AKI on the hippocampus. Renal IR injury has no effect on the hippocampus in the short term. *A* and *B*: microphotographs (×20 objective) of a H&E-stained hippocampus section (5 μm) for a representative control (*A*) and IR pig (*B*). *C*: immunofluorescence of a single representative section (5 μm) for a control and IR pig using DAPI to stain nuclei and a TUNEL Cell-Death Detection Kit (Roche) to fluorescently label apoptotic nuclei. *D*: semiquantitative pathologist score of mild-moderate lesions in the hippocampus.

liver transferase enzymes over the first 24–48 h of reperfusion (e.g., AST:ALT ratio, ALP; Fig. 1, *A*, *B*, and *C*). Other markers of acute liver injury were unaffected: plasma bilirubin, 3.24 vs. 3.84 ± 0.77 μmol/l, $P = 0.26$; GLDH, 1.75 vs. 2.19 ± 0.25 IU/l, $P = 0.10$ and GGT, 39.7 vs. 31.4 ± 5.5 IU/l, $P = 0.14$ for control vs. IR, respectively. Histopathological assessment of the liver by brightfield microscopy revealed no significant hepatocyte lesions (Fig. 1*D*). All described hepatocyte changes

Table 2. *Porcine hematology before, and ≤24 h after, renal ischemia-reperfusion injury*

	Treatment			Time						Statistics (*P* Value)		
	Control	IR	SED	0	2	4	6	24	SED	Treatment	Time	Treatment × time
Red cell number/mm^3	6.01	6.32	0.37	5.86	6.24*	6.31*	6.17*	6.25*	0.12	0.40	<.001	0.35
Red cell volume, μm^3	51.0	49.2	1.3	50.5	49.9	49.9	50.1	50.0	0.25	0.18	0.07	0.81
Hematocrit, %	30.6	31.0	1.5	29.5	31.1	31.5*	30.8	31.2	0.63	0.77	<.001	0.41
Hemoglobin, g/dl	10.8	10.4	0.49	10.1	10.7*	10.8*	10.7*	10.7*	0.23	0.49	<.001	0.66
Platelet cell number/mm^3	282	307	49	258	250	375*	271	335*	41	0.66	0.02	0.23
White cell number/mm^3	20.8	18.6	3.0	16.2	17.5	22.8	23.4	18.9	1.7	0.47	0.94	0.43

Data are for control (i.e., sham-operated; $n = 6$ female pigs) and IR ($n = 11$ female pigs) and are presented as means with average SE of the differences between means (SED) to represent the residual error. Porcine hematology before and after renal ischemia-reperfusion (IR) injury suggests no overt changes in blood cell count as a result of the treatment but a number of biologically small, but statistically significant, temporal changes with time. Whole blood was collected before (*time 0*) and after (2, 4, 6, 24 h) induction of 40-min renal IR injury. REML analysis was performed with treatment (control vs. IR) and time as fixed effects, using the individual animal as a nested random term in the model (Genstat v16). Where a statistically significant main effect was indicated ($P < 0.05$), then further post hoc 1-way analyses were conducted to indicate an effect of treatment or time (*row factor, indicates values that are different within same row). Confidence intervals (95%) may be estimated as ±2 SED.

were mild and were likely incidental or artifacts as a result of tissue processing. Fluorescence microscopy for intralobular hepatocyte apoptosis indicated no treatment effects ($TUNEL^{+ve}$ cells/FOV; 1.99 vs. 2.74 ± 1.6 cells for control vs. IR, respectively; Fig. 1*E*). Gene expression data for selected markers of early-stage hepatic cell injury, including apoptosis (caspase-3, Fig. 1*F*) or activation of proinflammatory cytokines (TNFα; Fig. 1*G*) or growth factors [transforming growth factor (TGF)-β1, Fig. 1*H*], were also negative. Similarly, AKI had no effect on lung tissue water content (Fig. 2*A*) or gross histopathology (Fig. 2, *B* and *C*). Histopathological examination indicated that all described lesions were mild to moderate, and combining data for all types of lesions observed (bronchopneumonia, bronchointerstitial pneumonia, and bronchial-associated lymphoid tissue hyperplasia) suggested no effect of IR-AKI (df_1, likelihood ratio = 1.04, F = 0.32). In most lung sections, mild-to-moderate numbers of interstitial eosinophils were observed, but this was considered a nonpathological incidental finding. Apoptotic cells were sporadically found at a low level throughout lung tissue (Fig. 2*D*), but no consistent

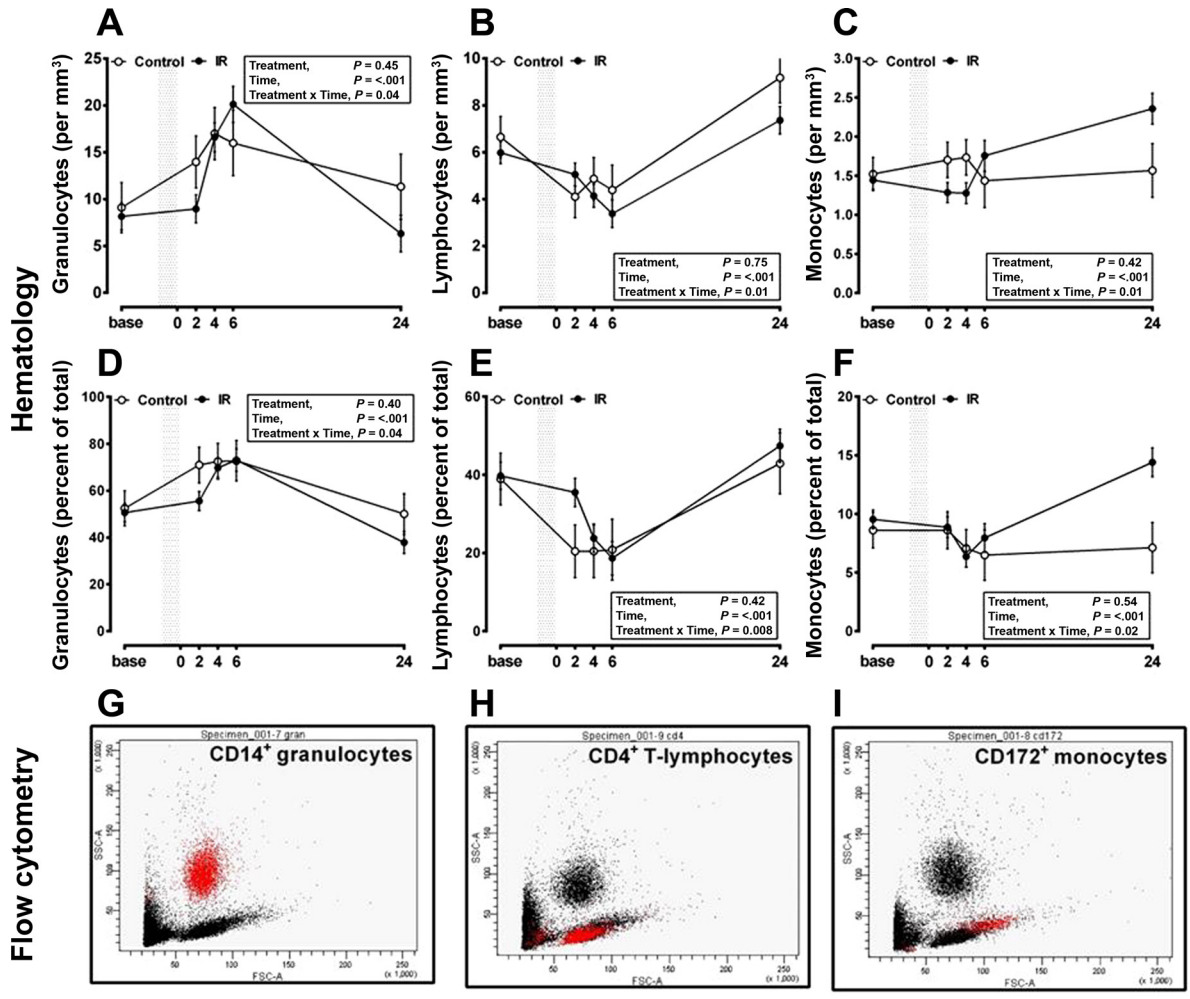

Table. Porcine haematology before, and up to 24h after, renal ischemia-reperfusion injury

	Treatment			Time						*Statistics (P-value)*		
	Control	IR	s.e.d.	0	2	4	6	24	s.e.d.	Treat	Time	Treatment × Time
CD4⁺ lymphocytes (percent of total)	6.01	6.32	0.37	5.86	6.24	6.31	6.17	6.25	0.12	0.40	<.001	0.35
CD172a⁺ monocytes (percent of total)	51.0	49.2	1.3	50.5	49.9	49.9	50.1	50.0	0.25	0.18	0.001	0.81
Granulocytes (percent of total)	30.6	31.0	1.5	29.5	31.1	31.5	30.8	31.2	0.63	0.77	<.001	0.41

Fig. 4. AKI in the pig has no overt effect on hematological parameters. *A–F*: hematology was conducted on fresh blood using a Medonics CA620 (Menarini; Wokingham, UK). *G–I*: flow cytometry was conducted on a BD-FACS Aria using mouse anti-pig FITC antibodies for neutrophil-derived granulocytes (ID: MCA2599F), monocyte-derived dendritic cells (CD172a+, ID: MCA2312F), or total lymphocytes ($CD4a^+$, ID: MCA1749F) all purchased from AbD Serotec, Kidlington, UK. The table at the *bottom* shows quantification of cell types after sham-surgery (control) or AKI (IR). Horizontal lines are mean with vertical lines ± ESE for control (n = 6) and IR (n = 11). Flow cytometry was conducted in n = 3 control or IR pigs, sampled serially to 24 h. Quantitative data were analyzed by ANOVA for the fixed effect of treatment (control vs. IR) with or without time as a within-animal repeated measure, as appropriate. Statistical significance was accepted at $P < 0.05$.

increase as a result of IR-AKI was noted. Hippocampal tissue was also assessed visually by brightfield (H&E) and fluorescence microscopy for histopathological abnormalities and apoptotic nuclei after IR-AKI: gross histology appeared normal (Fig. 3*A*), and the number of TUNEL^{+ve} cells was very low and not affected by AKI (TUNEL^{+ve} cells/FOV; 0.05 vs. 0.08 ± 0.5 cells for control vs. IR, respectively; Fig. 3*B*). In addition, the pathologists reported that most of the lesions observed (extracellular vacuolization, spongiosis, presence of dark neurons) were likely artifactual as a result of tissue processing. Combining data of all lesions for analysis indicated no effect of AKI (df_1, likelihood ratio = 0.26, F = 0.62; Fig. 3*D*).

Porcine Hematology and Tissue Cytokines After Renal IR Injury

Mild-moderate IR AKI had little effect on white blood cell, platelet, or red cell parameters in porcine whole blood, but some biologically small, yet statistically significant, temporal changes with time were noted (Table 2). AKI induced some changes in white blood cell count that were greater than observed in sham-control animals (Fig. 4, *A–F*), but the overall effects were small and not of appreciable biological significance. Using flow cytometry to quantify more accurately changes in specific populations of T-helper white blood cells (Fig. 4, *G–I*) confirmed no clear increase in numbers of neutrophil-derived granulocytes, CD4a$^+$ lymphocytes, or monocyte-derived dendritic cells (Fig. 4*J*). At 48 h after IR injury, the concentration of tissue cytokines was assessed in lysates of the kidney, liver, and lung. IR AKI had no effect on tissue cytokine concentrations in the kidney, liver, or lung. All organs had particularly high concentrations of IL-18 and IFN-γ (Table 3), and the relative total tissue concentration of all cytokines was liver >> kidney > lung (Fig. 5*C*). Toluidine blue staining for mast cell activation in AKI kidneys was negative for all sections examined (Fig. 5, *A* and *B*). Immunofluorescence for SLA2 (MHC-class II cell surface marker) was more marked in the kidney vs. the liver (Fig. 5*D*), but relative abundance was similar between treatment groups (Fig. 5, *D* and *E*).

Porcine Organ Tissue Electrolyte and Trace Element Composition After Renal IR Injury

As expected, there were notable differences between organs in electrolyte and elemental composition. The kidney had the highest concentrations of magnesium, sodium, calcium, copper, selenium, and cesium, whereas iron, zinc, manganese, and molybdenum tended to accumulate in the liver and vanadium in the lung (Table 4). Concentrations of potassium, thallium, cobalt, and arsenic were similar among organs (Table 4). In the kidney, IR AKI led to accumulation of sodium (Fig. 6*A*) and strontium (Table 4), with a strong trend for greater accumulation of calcium (Fig. 6*B*) and magnesium (Table 4) at 48 h postinjury. In the short term (i.e., at 48 h), remote effects of ischemic AKI on organ elemental composition were noted in the lung (e.g., accumulation of calcium; Fig. 6*B*) and in the liver (e.g., accumulation of molybdenum; IR, 3.40 ± 0.13 vs. control, 2.88 ± 0.15 μg/g DM; P = 0.01). Longer term follow-up of animals post-IR injury (at 5 wk) indicated that each effect noted above had resolved by 5 wk (Table 5, Fig. 6, *C* and *D*).

Remote Effects of AKI on Histopathology of the Liver and Lung at 5 Weeks Post-Ischemic Injury

At 5 wk post-ischemic injury, blood creatinine was not different between treatment groups [133 (123–137) vs. 130 (127–134) μmol/l, median (IQR) for control vs. IR pigs]. Similarly, hepatic transaminase enzyme levels were also not different between groups at this time [ALT, 30 (27–31) vs. 25 (24–26) IU/l; ALP, 100 (93–149) vs. 87 (80–106) IU/l; AST, 43 (34–43) vs. 23 (23–33) IU/l; median (IQR) for control vs. IR pigs, P = not significant (NS) all cases]. There was no evidence of residual edema in either tissue [% water in liver, 73.6 (72.7–73.7) vs. 75.2 (74.4–75.2); % water in lung, 81.5 (78.5–81.6) vs. 82.3 (81.7–82.5); median (IQR) for control vs. IR pigs, P = NS all cases], and tissue trace element composition was not different between treatment groups [e.g., cal-

Table 3. *Cytokine composition in the kidney, liver, and lung tissue lysates at 48 h after renal IR injury*

	Treatment			Tissue				Statistics (P Value)		
	Control	IR	SED	Kidney	Liver	Lung	SED.	Treatment	Tissue	Treatment × tissue
Lysate protein, mg/ml	20.9	21.0	1.6	17.0	29.5*	16.3	1.7	0.94	<.001	0.52
Cytokine, pg·ml^{-1}·mg protein^{-1}										
IFN-γ	0.781	0.718	0.215	0.942	0.556	ND	0.212	0.77		
IL-1α	0.008	0.007	0.001	0.012*	0.004	0.006	0.001	0.74	<.001	0.57
IL-1β	0.046	0.059	0.009	0.059	0.020*	0.060	0.009	0.19	<.001	0.32
IL-2	0.176	0.149	0.022	0.200	0.121*	0.160	0.019	0.26	<.001	0.78
IL-4	0.208	0.176	0.038	0.389	0.206	ND	0.037	0.42		
IL-6	0.004	0.004	0.001	0.005	0.002*	0.004	0.001	0.33	<.001	0.09
IL-8	0.033	0.031	0.003	0.064*	0.022	0.013	0.003	0.45	<.001	0.69
IL-10	0.013	0.011	0.001	0.023	0.015	0.002*	0.001	0.17	<.001	0.70
IL-12	0.009	0.008	0.001	0.013	0.004*	0.008	0.001	0.36	<.001	0.76
IL-18	0.820	0.930	0.079	0.880	0.721	1.05	0.138	0.17	0.06	0.35
TNF-α	0.001	0.001	0.000	0.003	0.000	ND	0.000	0.84		

Data are means ± SED for porcine kidney, liver, and lung tissue from control (n = 12) vs. IR (n = 17) groups. Cytokines were determined on organ tissue lysates using a porcine-specific Milliplex assay, in magnetic bead format (Milliplex PCYTMAG-23K, Merck Millipore). Values are corrected to tissue protein content. Data were analyzed by ANOVA for the fixed effects of IR, tissue, or their interaction using Genstat v16 (VSNi). Individual animal was incorporated as a nested, random term in the model to account for reduced variance of cytokines in the kidney, liver, and lung of the same animal. Where a statistically significant main effect was indicated ($P < 0.05$), then further post hoc 1-way analyses were conducted to indicate an effect of treatment or tissue (*row factor, indicates values that are different within same row). Confidence intervals (95%) may be estimated as ±2 SED. ND, Not detectable.

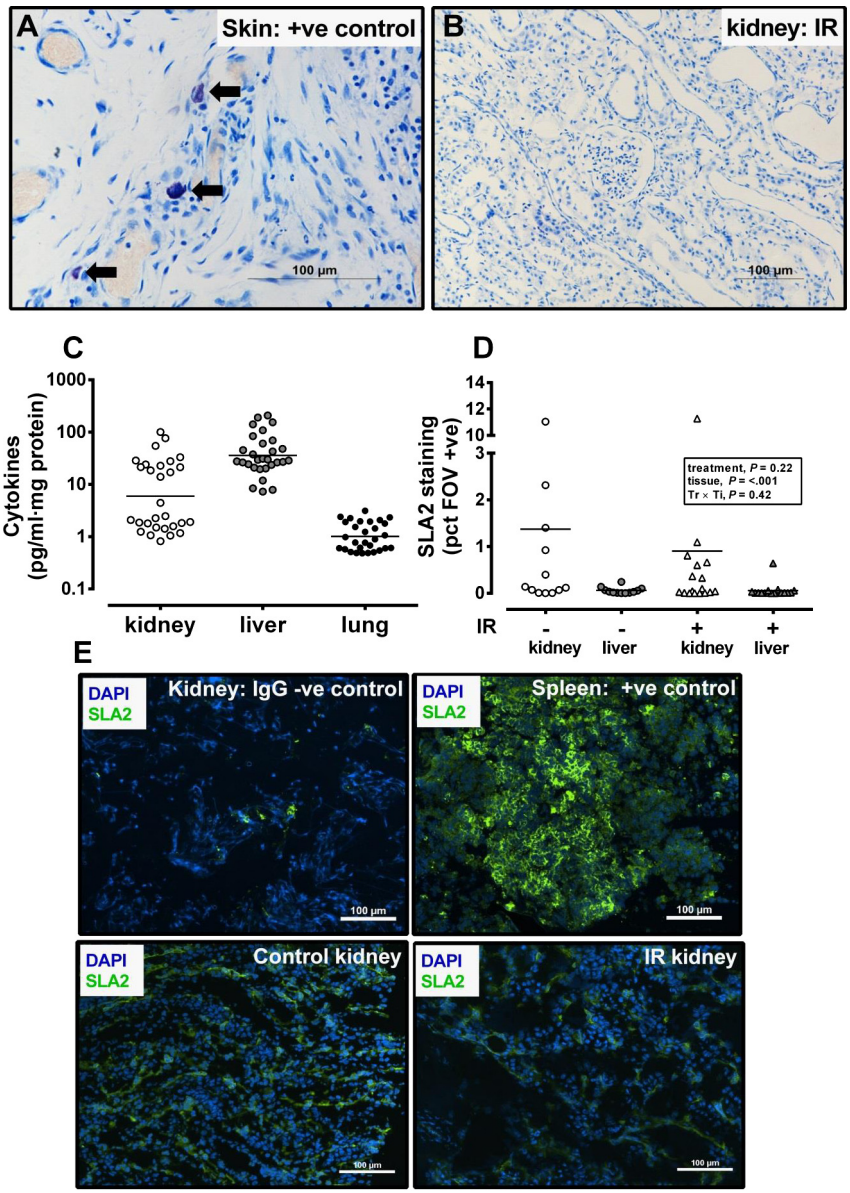

Fig. 5. AKI in the pig has no overt effect on tissue immune cell infiltration. *A* and *B*: microphotographs (×20 objective) of a toluidine blue-stained skin section from a dog (+ve control; sourced from pathology service, School of Veterinary Medicine and Science) and representative IR kidney section (5 μm). No kidney section from control ($n = 12$) or IR pigs ($n = 17$) was positive for activated mast cells. *C*: for comparative purposes, data are the sum of all measured cytokines ($pg \cdot ml^{-1} \cdot mg\ protein^{-1}$) for each animal in the kidney, liver, and lung. No effect of IR was noted for any cytokine within each organ (panel of 11 measured by Milliplex array; see METHODS). *D*: dot plot of quantification of swine leucocyte antigen 2 (SLA2) staining in sham-control vs. IR pigs. *E*: immunofluorescence of a single representative section (5 μm) for a control and IR pig using 4′,6-diamidino-2-phenylindole (DAPI) to stain nuclei and swine SLA2 to label all cells expressing MHC class II (DR region; AbD Serotec, Kidlington, UK). Control kidney and spleen were used as negative and positive controls, respectively. Quantitative data were analyzed by ANOVA for the fixed effect of treatment (control vs. IR) or tissue (kidney and liver), as appropriate. The individual pig was incorporated as a nested random (i.e., blocking factor) in the model to account for reduced intraindividual variation for the kidney, liver, and lung of the same individual. Horizontal line is at mean for each data set. Statistical significance was accepted at $P < 0.05$.

cium in liver, 131 (123–135) vs. 143 (132–152); calcium in lung, 274 (242–300) vs. 265 (255–278) mg/kg DM; median (IQR) for control vs. IR pigs, P = NS all cases]. At a time postinjury sufficient for any acute, subclinical remote organ injury to develop and manifest, no significant liver or lung histopathological lesions were observed in control or IR groups beyond those expected for pigs (Fig. 6, *E* and *F*). All described pulmonary and hepatocyte changes (e.g., lung; accumulation of intravascular alveolar leukocytes, intravascular thrombosis, bronchointerstitial pneumonia, BALT hyperplasia; liver; hepatocellular hydropic degeneration, extramedullary hematopoiesis) were categorized as mild, evenly distributed across groups and, again, were likely incidental findings.

DISCUSSION

We have shown that mild-moderate IR AKI increased calcium accumulation in the lung and increased plasma markers of acute hepatocyte damage. These relatively subtle changes occurred despite the absence of gross effects on remote organ histopathology or remote organ edema. Similarly, we observed no remote organ inflammatory cell infiltration or apoptosis at 48 h postischemic injury. We suggest that the remote organ effects of AKI widely reported using smaller animal models such as rodents are less likely to be representative of human disease. The reasons for the apparent increased susceptibility of smaller animals to remote organ damage are not clear but probably reflect the significant and obvious differences in anatomy and physiology vs. porcine and human organs. Local accumulation of major elements (e.g., sodium, magnesium) in the damaged kidney most likely contributes to the development of renal edema after AKI, as observed previously in this model (14).

Effects in the Lung

Many experimental studies have reported associations between AKI and respiratory complications (see Table 1 in Ref. 17). In one clinical study, the development of respira-

Table 4. *Major and trace element composition in kidney, liver, and lung tissue at 48 h after renal IR injury*

	Treatment			Tissue				Statistics (*P* Value)		
	Control	IR	SED	Kidney	Liver	Lung	SED	Treatment	Tissue	Treatment × tissue
Major elements, μg/g DM										
Potassium	13,026	13,167	396	13,192	12,269*	13,866	505	0.72	0.01	0.18
Magnesium	730	773	22	891*	698	676	29	0.07	<.001	0.08
Trace elements, μg/g DM										
Iron	340	318	31	127	504*	351	30	0.48	<.001	0.88
Zinc	159	158	9	121	267*	88	11	0.88	<.001	0.53
Copper	14.9	14.6	0.9	24.6	16.2	3.4*	1.2	0.78	<.001	0.13
Selenium	3.47	3.39	0.14	7.51*	1.61	1.15	0.18	0.61	<.001	0.57
Manganese	5.30	5.19	0.34	5.38	10.06*	0.27	0.39	0.76	<.001	0.17
Molybdenum	1.90	1.97	0.12	2.62	3.18	0.02*	0.13	0.55	<.001	0.01
Thallium	0.57	0.60	0.03	0.62	0.59	0.55	0.03	0.48	0.17	0.12
Strontium	0.09	0.18*	0.02	0.19	0.05*	0.18	0.03	0.003	<.001	0.14
Cobalt	0.02	0.02	0.003	0.03	0.03	0.002*	0.002	0.78	<.001	0.43
Arsenic	0.06	0.04	0.03	0.04	0.05	0.05	0.02	0.66	0.90	0.24
Cesium	0.04	0.05	0.007	0.07*	0.02	0.03	0.003	0.24	<.001	0.85
Vanadium	0.02	0.03	0.004	0.04	0.03*	0.009	0.005	0.22	<.001	0.50

Data are means ± SED for porcine kidney, liver, and lung tissue from control ($n = 12$) vs. IR ($n = 17$) groups. Major and trace elements were measured in a known mass of freeze-dried tissue (DM) after acid hydrolysis using inductively coupled plasma mass spectrometry (ICP-MS). Data were analyzed by ANOVA for the fixed effects of IR, tissue, or their interaction using Genstat v16 (VSNi). Where a statistically significant main effect was indicated ($P < 0.05$), then further post hoc 1-way analyses were conducted to indicate an effect of treatment or tissue (*row factor, indicates values that are different within same row).

tory failure, after contrast-induced AKI, was identified as a major contributing factor toward the five- to sixfold increase in mortality compared with patients who did not develop AKI after surgery, even after adjustment for comorbidities (29). Mechanisms underlying such respiratory failure appear to include effects on cellular ion pumps which result in extravasation of fluid and tissue edema, together with inflammatory infiltration (e.g., neutrophils, cytokines) (17) and apoptosis (20). Each of these contributing factors was assessed in the current study, together with detailed electrolyte and trace element analyses. Although we observed, for the first time, increased lung tissue concentration of calcium after AKI (Fig. 5*B*), the effects were biologically small. Without concurrent effects on other electrolytes such as sodium, potassium, or magnesium, the effect on calcium was not significant enough to alter pulmonary water content or histopathological indices of pulmonary damage. A fluid shift from intracellular to interstitial compartments cannot be ruled out, however. Despite clear differences in the pattern of cytokines and baseline levels of apoptosis between organs of the same animal, there was no obvious additional effect of AKI. Our data, therefore, do not completely discount potential adverse pulmonary effects of AKI. Age, gender (no males were analyzed), and the presence of other comorbidities, which were not represented in our study, may have considerable influence. The data do suggest, however, that experimental observations of AKI from rodent models may not necessarily be seen in larger animal models or humans. This may be due to allometry, in which acute diseases like AKI that have an energetic/mitochondrial etiology (10, 36), become less evident in animals with a larger surface area-to-body weight ratio (33).

Effects in the Liver

The majority of remote effects observed in the liver are from experimental, rather than clinical, studies and, as with the lung, relate to cell damage induced by increased cytokine and inflammatory cell influx (28). It has been suggested that this leads to increased appearance in the systemic circulation of enzymatic markers of acute liver injury after AKI, such as amino acid transferases (28). This response was notable in pigs in our study (Fig. 1, *A* and *B*) but also in another study using a rat model of renal ischemia (16). In both studies, hepatic enzyme levels returned to baseline by 24 h, indicating a short-term effect unlikely to affect liver function adversely. In contrast to the study of Golab et al. (16), we did not observe any significant association of hepatic enzymes with hepatocyte apoptosis or inflammatory cell infiltration in lobules. We do not necessarily discount a specific interaction between general anesthesia and kidney dysfunction on markers of acute liver cell injury, but our results do suggest that AKI has few major effects in the liver in otherwise healthy individuals. Ischemic AKI does appear to have a mild effect on the liver, but it remains to be seen whether this is clinically significant under some circumstances, e.g., in the presence of preexisting liver disease.

Fig. 6. AKI leads to short-term sodium and calcium accumulation in the kidney and calcium accumulation in the lung. At 5 wk post-IR injury, no significant histopathology or remote effects were noted. *A* and *B*: dot plot of total sodium or calcium in the kidney, liver, and lung for control vs. IR pigs at 48 h postinjury. *C* and *D*: dot plot of total sodium or calcium in the kidney, liver, and lung for control vs. IR pigs at 5 wk postinjury. Electrolytes were measured in dried tissue (dry matter; DM) after acid digestion by inductively coupled plasma mass spectrometry (see METHODS). Quantitative data were analyzed by ANOVA for the fixed effect of treatment (control vs. IR) or tissue (kidney, liver, and lung), as appropriate. The individual pig was incorporated as a nested random (i.e., blocking factor) in the model to account for reduced intraindividual variation for the kidney, liver, and lung of the same individual. Horizontal line is at mean for each data set. Statistical significance was accepted at $P < 0.05$. *C* and *D*: summary histopathological assessment report from 2 pathologists for the liver and lung.

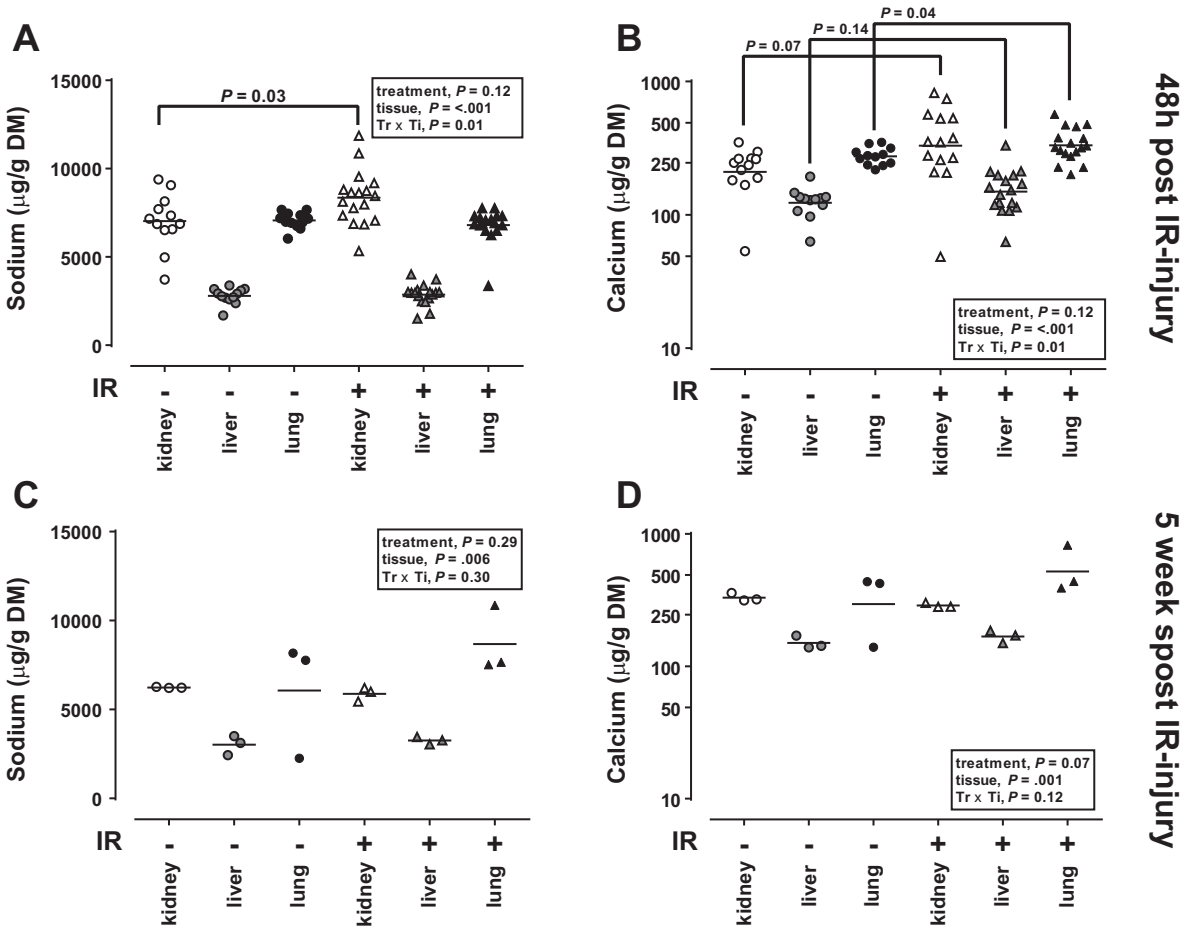

E

PULMONARY histopathologic assessmentat 5-weeks post ischemicinjury

		Histopathologic assessment category			
		Accumulation of intravascular alveolar leukocytes	Intravascular thrombosis	Bronchointerstitial pneumonia	BALT hyperplasia
Pig 1	Control	+	+	-	-
Pig 2	Control	+	-	-	-
Pig 3	Control	+	-	-	-
Pig 4	IR	+	-	+	-
Pig 5	IR	+	-	-	+
Pig 6	IR	+	-	-	-

Key to categories: Accumulation of intravascular alveolar leukocytes, mainly neutrophils, eosinophils and monocytes with rare megakaryocytes; Intravascular thrombosis, only in one medium-sized artery; slide quality, tissue was generally well-preserved. Lesions are graded by two pathologists (as: - (absence), + (mild), ++ (moderate) or +++ (severe).

F

HEPATIC histopathologic assessment at 5-weeks post ischemic injury

		Histopathologic assessment category	
		Hepatocellular hydropic degeneration	Extramedullary hematopoiesis
Pig 1	Control	+	+
Pig 2	Control	+	+
Pig 3	Control	+	+
Pig 4	IR	+	+
Pig 5	IR	+	+
Pig 6	IR	+	+

Key to categories: Hepatocellular hydropic degeneration: This is a non-specific reversible hepatocellular cytoplasmic swelling seen after various toxic and metabolic insults, hypoxia, and cholestasis. Slide quality, tissue was generally well-preserved. Lesions are graded by two pathologists (as: - (absence), + (mild), ++ (moderate) or +++ (severe). All examined tissue samples showed an almost identical microscopic appearance.

Table 5. *Major and trace element composition in kidney, liver, and lung tissue at 5 wk after renal IR injury*

	Treatment			Tissue				Statistics (*P* Value)		
	Control	IR	SED	Kidney	Liver	Lung	SED	Treatment	Tissue	Treatment × tissue
Major elements, μg/g DM										
Sodium	5,105	5,938	689	6,059	3,136*	7,370	944	0.29	0.006	0.30
Potassium	13,026	13,167	396	14,471	11,403*	14,357	505	0.72	0.01	0.18
Magnesium	728	759	23	929*	647	675	18	0.75	<.001	0.02
Calcium	271	345	45	309	159*	441	69	0.15	0.01	0.20
Trace elements, μg/g DM										
Iron	452	347	68	243	588*	367	56	0.11	<.001	0.66
Zinc	146	153	10	147	210	92*	11	0.46	<.001	0.34
Copper	26.2	23.5	2.1	42.8	27.4	4.2*	2.7	0.24	<.001	0.22
Selenium	3.98	3.95	0.15	8.68*	1.95	1.27	0.18	0.85	<.001	0.36
Manganese	6.33	6.30	0.52	7.84	9.83	1.27*	0.34	0.95	<.001	0.06
Molybdenum	2.95	2.67	0.29	3.85	4.00	0.56*	0.24	0.37	<.001	0.17
Cadmium	0.61	0.41	0.18	1.39*	0.12	0.02	0.09	0.04	<.001	0.01
Thallium	0.01	0.01	0.01	0.019	0.019	0.009*	0.001	0.33	<.001	0.12
Strontium	0.11	0.18*	0.02	0.18	0.06*	0.20	0.03	0.03	<.001	0.13
Cobalt	0.03	0.03	0.002	0.05	0.04	0.01*	0.003	0.57	<.001	0.04
Arsenic	ND	ND	—	ND	ND	ND				
Cesium	0.03	0.03	0.002	0.05	0.01*	0.02	0.002	0.71	<.001	0.02
Vanadium	0.01	0.02	0.009	0.01	0.01	0.01	0.013	0.14	0.85	0.12

Data are means ± SED for porcine kidney, liver and lung tissue from control ($n = 3$) vs. IR ($n = 3$) pigs at 5 wk post-ischemic injury. Major and trace elements were measured in a known mass of freeze dried tissue after acid hydrolysis using ICP-MS. Data were analyzed by ANOVA for the fixed effects of IR, tissue, or their interaction using Genstat v16 (VSNi). Where a statistically significant main effect was indicated ($P < 0.05$), then further post hoc 1-way analyses were conducted to indicate an effect of treatment or tissue (*row factor, indicates values that are different within same row). ND, below detectable limits (0.01 ppb.)

Effects in the Brain

In this study, we chose the hippocampus as a discrete brain region that, in models of global cerebral ischemia, appears highly susceptible to IR injury. The CA1, CA3, and dentate gyrus regions appear to be particularly susceptible (26). Neurological sequelae of AKI are well documented and include decreased mental status, seizures, and encephalopathy. In mouse models, significant cerebral effects such as neuronal pyknosis and microgliosis in the hippocampus have been noted (30). However, in our study, histopathological examination revealed no consistent adverse effects related to AKI. Immunofluorescence of $TUNEL^{+ve}$ hippocampal cells suggested very low levels in controls, which were not exacerbated by AKI. We did not assess tissue cytokine concentrations in the brain, but lack of significant accumulation in other more susceptible organs suggests that the brain might only have basal levels, near to the limit for detection. A subjective, behavioral scoring system was developed in-house to assess adequacy of postoperative recovery. This included species-specific indices of pain, alertness, and food and water consumption. AKI pigs exhibited obtundation for 4–8 h postsurgery in contrast to 1–3 h in sham-controls, but the symptoms were typical of an azotemic animal rather than indicative of remotely induced cerebral disease.

Effects on the Kidney

We have previously described and characterized ischemic AKI in our pig model (14) but extend these observations here to include further examination of possible intrarenal (cortex) immune cell infiltration, electrolyte, and elemental disturbance. As seen in the lung, the accumulation of electrolytes in renal tissue (Na^+, Ca^{2+}; Fig. 5, *A* and *B*) probably contributes to renal edema after AKI (14). Investigating a possible immunological basis for AKI in our porcine model, we saw no greater cytokine infiltration of renal tissue when assessed histologically and by cytokine array (Table 3). Furthermore, there was *1*) no increase in mast cell activation (marking entry for activation of the complement pathway; Fig. 4, *A* and *B*); *2*) no increased presentation of the MHC class-II cell surface marker (SLA-2 immunofluorescence; Fig. 4, *D* and *E*), nor *3*) any increase in white cell count in whole blood postsurgery (Table 2, Fig. 3). Absence of any sterile inflammatory response in renal tissue in this study may be partially attributable to the time scale of the study (2 days). It is possible that examination after 5–7 days would have demonstrated an alternative wave of immune cell infiltration (38). However, given the extent of decline in kidney function, marked by azotemia (100–150% increase in plasma creatinine and urea), associated with tissue damage as early as 24 h postsurgery (14), we might have expected to observe at least some evidence of increased granulocytes in blood or increased numbers of neutrophils in kidney tissue by 48 h, but neither was evident (22). Any immune cell infiltration observed by pathologists in this study tended to be lymphocytic. Again, this contrasts with rodent models, in which a well-characterized sterile inflammatory response is seen in association with AKI, within a similar time frame to our study (2, 3, 40). We assume that species differences exist in the immunological response to AKI (39). Evidently, choice of an animal model is very important with respect to translation to the clinical situation. It is also likely to be of fundamental importance in related biomedical contexts such as drug development and evaluation. Finally, it is of interest that examination of the multiorgan profile of tissue cytokines illustrates different patterns between organs, the kidney having a particularly high concentration of IL-18 (Table 3). IL-18 has been proposed as a urinary biomarker for AKI (35), and our study suggests that this might be due to an accumulation of IL-18 within renal tissue and loss into urine following local cell damage or necrosis.

In summary, we investigated potential remote organ effects of AKI in a preclinical porcine model. The degree of kidney damage induced by our approach, reported here and previously (14), is consistent with KDIGO Stage 1/2 established clinically. Nevertheless, AKI had only subtle biochemical effects on distant organ tissues (e.g., the liver), which may account for transient increments in markers of cell damage in organs (e.g., liver transferases). We report no evidence of significant remote organ histopathology, cellular apoptosis, tissue edema, or increased immune cell infiltration after AKI. We accept that our porcine model of AKI has some limitations: we use young, healthy female animals with only a relatively short-term follow-up. Previous reports suggest females are relatively "protected" against myocardial (23) and renal (13) ischemic injury. However, the female pigs in our model suffer moderate renal damage, azotemia, and an increase in IL-1β (14), effects not consistent with abrogation of AKI. Furthermore, many studies have reported remote-organ effects as early as 6 h postinjury (19), with many demonstrating marked effects at 24 h (27). Hence, using our large-animal model of defined mild-moderate acute kidney damage (14), without significant baseline comorbidities, allows us to study the isolated effect of AKI in an animal with similar organ anatomy and physiology to humans. Choice of an animal model is of utmost importance for preclinical, in particular AKI, research (8). We do not discount that, clinically, remote organ effects may occur after AKI. However, such effects are likely exacerbated by the presence of multiple comorbidities or advanced age at admission.

ACKNOWLEDGMENTS

The authors gratefully acknowledge help and support from the Biomedical Services Unit on the Sutton Bonington Campus, University of Nottingham, and Jim Craigon for statistical advice on the manuscript.

GRANTS

This study was funded by the Faculty of Medicine, School of Veterinary Medicine and Science and School of Medicine, University of Nottingham and by Nottingham University Hospitals NHS Trust Charities.

DISCLOSURES

No conflicts of interest, financial or otherwise, are declared by the authors.

AUTHOR CONTRIBUTIONS

Author contributions: D.S.G. provided conception and design of research; D.S.G., S.D.B., L.J.D., L.G.R., S.J.W., R.F., S.E.O., and W.O. performed experiments; D.S.G. analyzed data; D.S.G., S.D.B., L.G.R., S.J.W., and M.A.D. interpreted results of experiments; D.S.G. prepared figures; D.S.G. drafted manuscript; D.S.G., S.D.B., L.G.R., and M.A.D. edited and revised manuscript; D.S.G., S.D.B., L.J.D., L.G.R., S.J.W., R.F., S.E.O., W.O., and M.A.D. approved final version of manuscript.

REFERENCES

1. **Archer SL.** Mitochondrial dynamics—mitochondrial fission and fusion in human diseases. *N Engl J Med* 369: 2236–2251, 2013.
2. **Bellomo R, Kellum JA, Ronco C.** Acute kidney injury. *Lancet* 380: 756–766, 2012.
3. **Bonventre JV, Yang L.** Cellular pathophysiology of ischemic acute kidney injury. *J Clin Invest* 121: 4210–4221, 2011.
4. **Carden DL, Granger DN.** Pathophysiology of ischaemia-reperfusion injury. *J Pathol* 190: 255–266, 2000.
5. **Chawla LS, Eggers PW, Star RA, Kimmel PL.** Acute kidney injury and chronic kidney disease as interconnected syndromes. *N Engl J Med* 371: 58–66, 2014.
6. **Chou AH, Lee CM, Chen CY, Liou JT, Liu FC, Chen YL, Day YJ.** Hippocampal transcriptional dysregulation after renal ischemia and reperfusion. *Brain Res* 25: 197–210, 2014.
7. **Coca SG, Singanamala S, Parikh CR.** Chronic kidney disease after acute kidney injury: a systematic review and meta-analysis. *Kidney Int* 81: 442–448, 2012.
8. **de Caestecker M, Humphreys BD, Liu KD, Fissell WH, Cerda J, Nolin TD, Askenazi D, Mour G, Harrell FE, Pullen N, Okusa MD, Faubel S; ASN AKI Advisory Group.** Bridging translation by improving preclinical study design in AKI. *J Am Soc Nephrol* 26: 2905–2916, 2015.
9. **Else PL, Hulbert AJ.** An allometric comparison of the mitochondria of mammalian and reptilian tissues: the implications for the evolution of endothermy. *J Comp Physiol B* 156: 3–11, 1985.
10. **Else PL, Hulbert AJ.** Mammals: an allometric study of metabolism at tissue and mitochondrial level. *Am J Physiol Regul Integr Comp Physiol* 248: R415–R421, 1985.
11. **Eltzschig HK, Carmeliet P.** Hypoxia and inflammation. *N Engl J Med* 364: 656–665, 2011.
12. **Faubel S.** Pulmonary complications after acute kidney injury. *Adv Chronic Kidney Dis* 15: 284–296, 2008.
13. **Fekete A, Vannay Á, Vér Á, Vásárhelyi B, Müller V, Ouyang N, Reusz G, Tulassay T, Szabó AJ.** Sex differences in the alterations of Na^+,K^+-ATPase following ischaemia-reperfusion injury in the rat kidney. *J Physiol* 555: 471–480, 2004.
14. **Gardner DS, Welham SJ, Dunford LJ, McCulloch TA, Hodi Z, Sleeman P, O'Sullivan S, Devonald MA.** Remote conditioning or erythropoietin before surgery primes kidneys to clear ischemia-reperfusion-damaged cells: a renoprotective mechanism? *Am J Physiol Renal Physiol* 306: F873–F884, 2014.
15. **Giraud S, Favreau F, Chatauret N, Thuillier R, Maiga S, Hauet T.** Contribution of large pig for renal ischemia-reperfusion and transplantation studies: the preclinical model. *J Biomed Biotechnol* 2011: 532127, 2011.
16. **Golab F, Kadkhodaee M, Zahmatkesh M, Hedayati M, Arab H, Schuster R, Zahedi K, Lentsch AB, Soleimani M.** Ischemic and non-ischemic acute kidney injury cause hepatic damage. *Kidney Int* 75: 783–792, 2009.
17. **Grams ME, Rabb H.** The distant organ effects of acute kidney injury. *Kidney Int* 81: 942–948, 2012.
18. **Gray C, Al-Dujaili EA, Sparrow AJ, Gardiner SM, Craigon J, Welham SJ, Gardner DS.** Excess maternal salt intake produces sex-specific hypertension in offspring: putative roles for kidney and gastrointestinal sodium handling. *PLoS One* 8: e72682, 2013.
19. **Grigoryev DN, Liu M, Hassoun HT, Cheadle C, Barnes KC, Rabb H.** The local and systemic inflammatory transcriptome after acute kidney injury. *J Am Soc Nephrol* 19: 547–558, 2008.
20. **Hassoun HT, Lie ML, Grigoryev DN, Liu M, Tuder RM, Rabb H.** Kidney ischemia-reperfusion injury induces caspase-dependent pulmonary apoptosis. *Am J Physiol Renal Physiol* 297: F125–F137, 2009.
21. **Hobson CE, Yavas S, Segal MS, Schold JD, Tribble CG, Layon AJ, Bihorac A.** Acute kidney injury is associated with increased long-term mortality after cardiothoracic surgery. *Circulation* 119: 2444–2453, 2009.
22. **Jang HR, Rabb H.** Immune cells in experimental acute kidney injury. *Nat Rev Nephrol* 11: 88–101, 2015.
23. **Johnson MS, Moore RL, Brown DA.** Sex differences in myocardial infarct size are abolished by sarcolemmal K_{ATP} channel blockade in rat. *Am J Physiol Heart Circ Physiol* 290: H2644–H2647, 2006.
24. **Kelly KJ.** Distant effects of experimental renal ischemia/reperfusion injury. *J Am Soc Nephrol* 14: 1549–1558, 2003.
25. **Kerr M, Bedford M, Matthews B, O'Donoghue D.** The economic impact of acute kidney injury in England. *Nephrol Dial Transplant* 29: 1362–1368, 2014.
26. **Koehler RC.** Pathogenic mechanisms of brain injury following global cerebral ischaemia. In: *Acute Stroke: Bench to Bedside*, edited by Bhardwaj A, Kirsch NJ, and Traystman JR. New York: Informa Healthcare, 2007, p. 293–312.
27. **Kramer AA, Postler G, Salhab KF, Mendez C, Carey LC, Rabb H.** Renal ischemia/reperfusion leads to macrophage-mediated increase in pulmonary vascular permeability. *Kidney Int* 55: 2362–2367, 1999.
28. **Lane K, Dixon JJ, MacPhee IAM, Philips BJ.** Renohepatic crosstalk: does acute kidney injury cause liver dysfunction? *Nephrol Dial Transplant* 28: 1634–1637, 2013.
29. **Levy EM, Viscoli CM, Horwitz RI.** The effect of acute renal failure on mortality: a cohort analysis. *JAMA* 275: 1489–1494, 1996.

30. **Liu M, Liang Y, Chigurupati S, Lathia JD, Pletnikov M, Sun Z, Crow M, Ross CA, Mattson MP, Rabb H.** Acute kidney injury leads to inflammation and functional changes in the brain. *J Am Soc Nephrol* 19: 1360–1370, 2008.
31. **Lunney JK.** Advances in swine biomedical model genomics. *Int J Biol Sci* 3: 179–184, 2007.
32. **Mason J, Beck F, Dorge A, Rick R, Thurau K.** Intracellular electrolyte composition following renal ischemia. *Kidney Int* 20: 61–70, 1981.
33. **Nunnari J, Suomalainen A.** Mitochondria: in sickness and in health. *Cell* 148: 1145–1159, 2012.
34. **Paladino JD, Hotchkiss JR, Rabb H.** Acute kidney injury and lung dysfunction: a paradigm for remote organ effects of kidney disease? *Microvasc Res* 77: 8–12, 2009.
35. **Parikh CR, Abraham E, Ancukiewicz M, Edelstein CL.** Urine IL-18 is an early diagnostic marker for acute kidney injury and predicts mortality in the intensive care unit. *J Am Soc Nephrol* 16: 3046–3052, 2005.
36. **Porter RK, Hulbert AJ, Brand MD.** Allometry of mitochondrial proton leak: influence of membrane surface area and fatty acid composition. *Am J Physiol Regul Integr Comp Physiol* 271: R1550–R1560, 1996.
37. **Prather RS, Lorson M, Ross JW, Whyte JJ, Walters E.** Genetically engineered pig models for human diseases. *Annu Rev Anim Biosci* 1: 203–219, 2013.
38. **Rock KL, Latz E, Ontiveros F, Kono H.** The sterile inflammatory response. *Annu Rev Immunol* 28: 321–342, 2010.
39. **Seok J, Warren HS, Cuenca AG, Mindrinos MN, Baker HV, Xu W, Richards DR, McDonald-Smith GP, Gao H, Hennessy L, Finnerty CC, López CM, Honari S, Moore EE, Minei JP, Cuschieri J, Bankey PE, Johnson JL, Sperry J, Nathens AB, Billiar TR, West MA, Jeschke MG, Klein MB, Gamelli RL, Gibran NS, Brownstein BH, Miller-Graziano C, Calvano SE, Mason PH, Cobb JP, Rahme LG, Lowry SF, Maier RV, Moldawer LL, Herndon DN, Davis RW, Xiao W, Tompkins RG; Inflammation and Host Response to Injury, Large Scale Collaborative Research Program.** Genomic responses in mouse models poorly mimic human inflammatory diseases. *Proc Natl Acad Sci USA* 110: 3507–3512, 2013.
40. **Sharfuddin AA, Molitoris BA.** Pathophysiology of ischemic acute kidney injury. *Nat Rev Nephrol* 7: 189–200, 2011.
41. **Sponsel HT, Alfrey AC, Hammond WS, Durr JA, Ray C, Anderson RJ.** Effect of iron on renal tubular epithelial cells. *Kidney Int* 50: 436–444, 1996.
42. **Zager RA, Burkhart K.** Myoglobin toxicity in proximal human kidney cells: roles of Fe, Ca^{2+}, H_2O_2, and terminal mitochondrial electron transport. *Kidney Int* 51: 728–738, 1997.